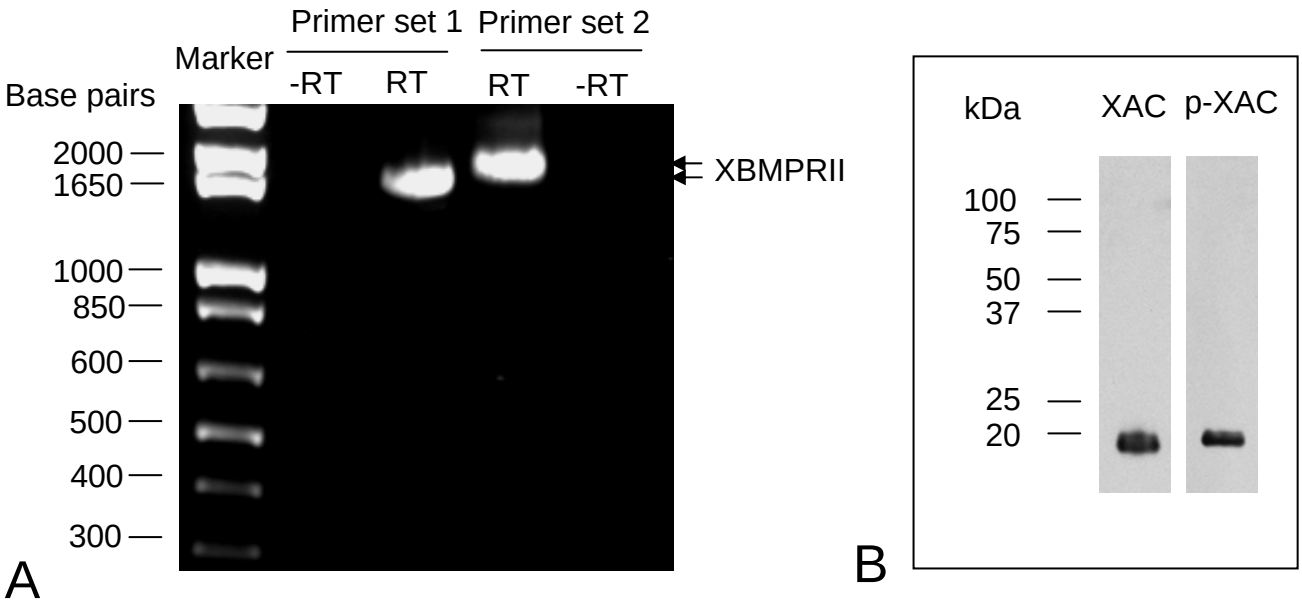

Supplemental figure 1. PCR analysis of BMPRII expression and western blotting of ADF/cofilin in *Xenopus* neural tube tissues. (**A**). Expression of the long form of BMPRII in *Xenopus* neural tube tissues. RT-PCR using two different primer sets on purified *Xenopus* neural tubes detects only the long form of BMPRII. Sequencing of the PCR products confirms that they are the long form XBMPRII. (**B**). Western blot analysis using XAC and p-XAC antibodies detects a predominant band in 2 µg *Xenopus* whole embryo cell lysates.

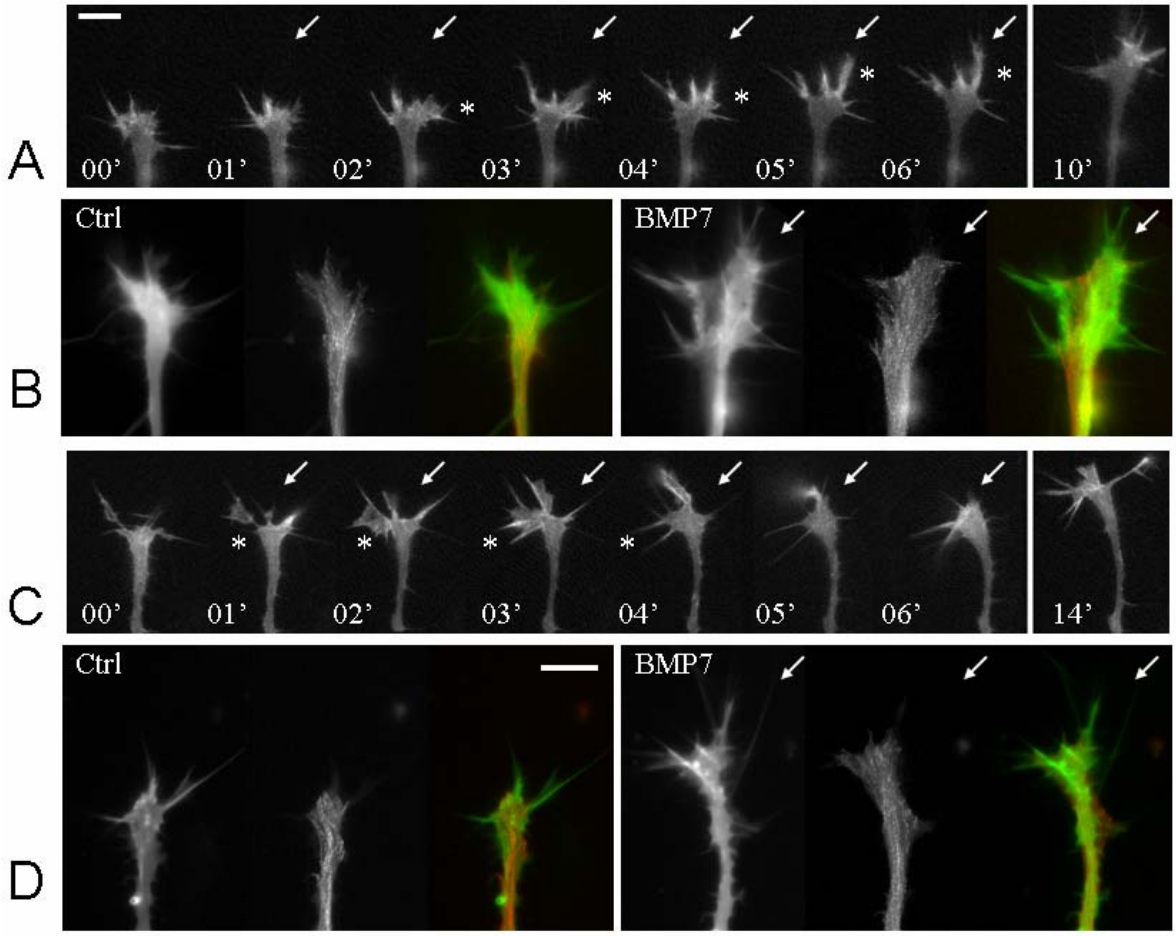

Supplemental figure 2. Fluorescence live imaging of GFP-γ-actin and mRFP-EB3 in *Xenopus* growth cones during attraction and repulsion. (**A**-**B**) A *Xenopus* growth cone from 6 hr cultures exhibited attractive turning to the BMP7 gradient. The GFP-γ-actin and mRFP-EB3 were imaged simultaneously through the use of DualView (Optical Insights), but only the GFP-γ-actin is shown here as a time-lapse sequence (A). The arrow indicates the onset of the BMP7 gradient. Time (min) in the BMP7 gradient is shown. Asterisks mark the local protrusion of lamellipodia and filopodia. To better show the asymmetric distribution, Z-projected images of the growth cone from the time-lapse sequences of both GFP-γ-actin and mRFP-EB3 from the control period (left) and the BMP7 application period (right) are shown in (B). For each panel, the z-projected GFP-actin (left), mRFP-EB3 (middle), and their color merge (right; green: GFP-γ-actin, red: mRFP-EB3) are presented. Arrows indicate the BMP7 gradient. (**C**-**D**) A *Xenopus* growth cone from the overnight culture was repelled by the BMP7 gradient. The BMP7 gradient inhibited the proximal actin-based protrusive activity, but permitted protrusion on the distal side of the growth cone (C; asterisks). At the end of 15 min, the growth cone grew and turned away from the BMP7 gradient (C). To summarize the change in distribution, Z-projected images of the growth cone from the time-lapse sequences of both GFP-γ-actin and mRFP-EB3 from the control period (left) and the BMP7 application period (right) are shown in (D). For each panel, the z-projected GFP-γ-actin (left), mRFP-EB3 (middle), and their color merge (right; green: GFP-γ-actin, red: mRFP-EB3) are presented. Arrows indicate the BMP7 gradient. Scale bar =10 μm. The complete time-lapse sequences of these two growth cones are included as Supplementary Video Clips (see below).

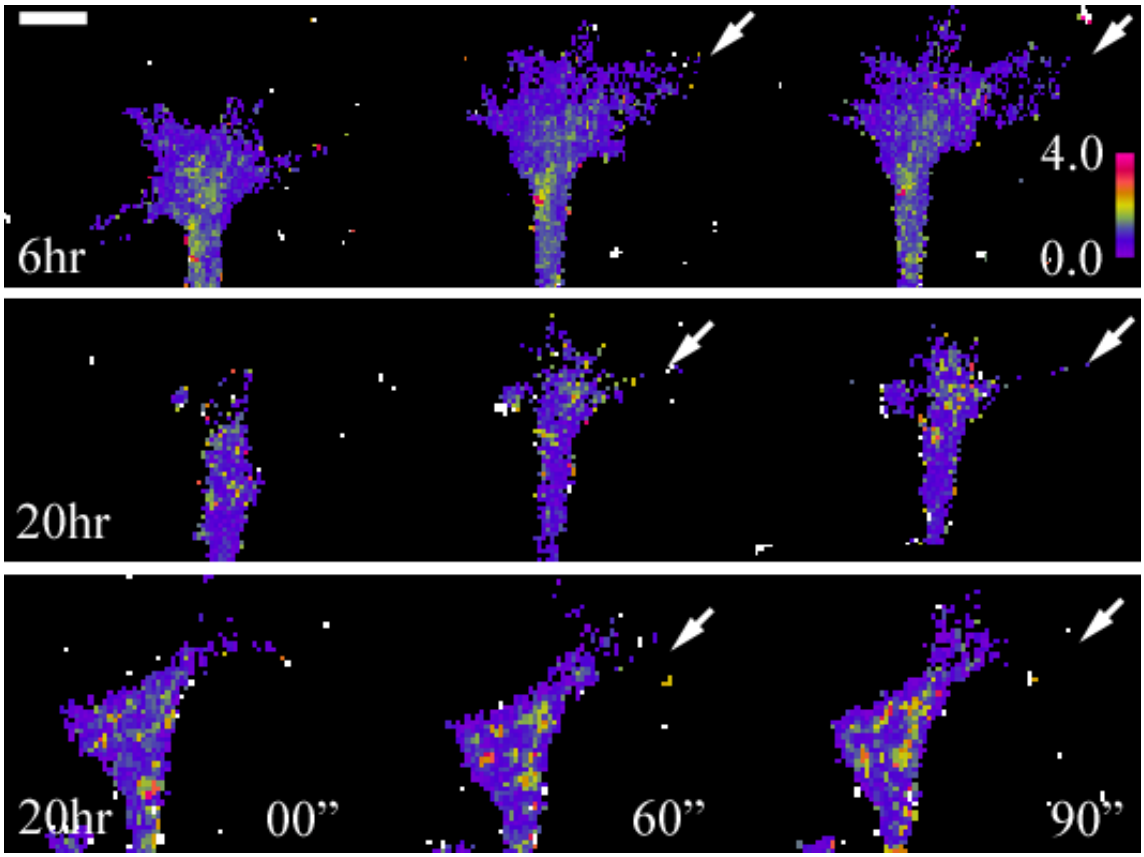

Supplemental figure 3. Ratiometric Ca^{2+} images of growth cones in response to the BMP7 gradient. The top row indicates a growth cone from 6 hr cultures, and the bottom two rows show two growth cones from 20 hr cultures. The arrows indicate the direction of the BMP7 gradients. Relative changes in the fluo-4/fura-red ratio are encoded by pseudocolors.. The scale bar is 10 μm. All the images were acquired using a Nikon C1 confocal and both fluorescent dyes were excited by 488 nM Argon laser (see the main text).

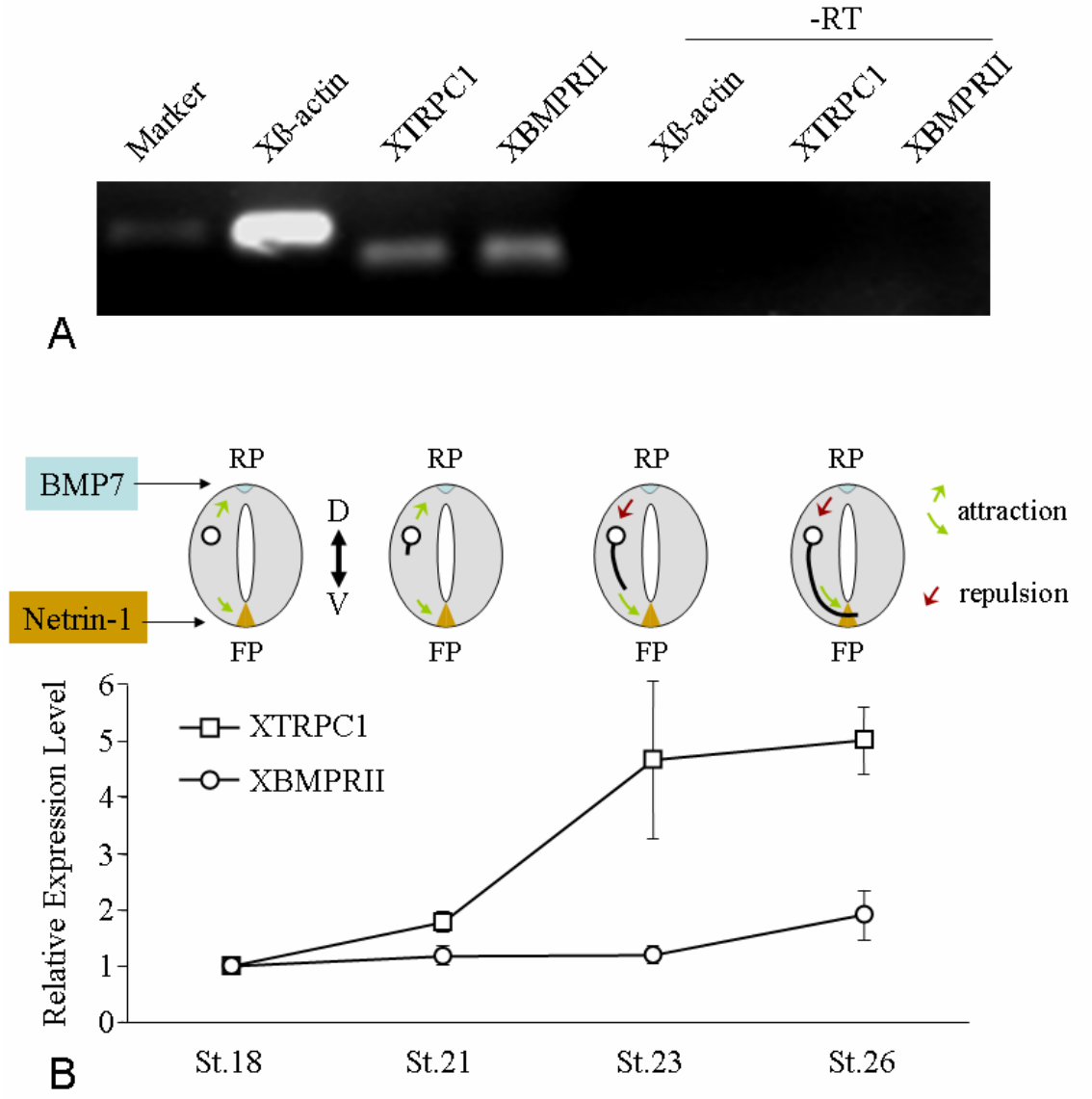

Supplemental figure 4. Real time PCR analysis of the expression profile of XTRPC1 and XBMPRII in *Xenopus* neural tubes. (**A**) Primers specific to *Xenopus* β -actin, XTRPC and XBRII are designed by PrimerExpress software and tested in RT-PCR using RNA sample from Stage 26 *Xenopus* neural tube tissues. -RT: RNA sample without reverse transcriptase. (**B**) Quantitative real-time PCR was performed using the SYBR Green system (Applied Biosystems, Foster City, CA) and the data were normalized by the expression level of β-actin. The RNA expression level of the stage 18 neural tube tissues was set as 1. Different stages of developing *Xenopus* embryos and their correlations with the specific stage of commissural axon projection are depicted in the schematic diagram, basing on the published results (Moon et al. 2005, *Dev Biol*. 288:474-86; Shim et al. 2005, *Nat Neurosci*. 8:730-5).

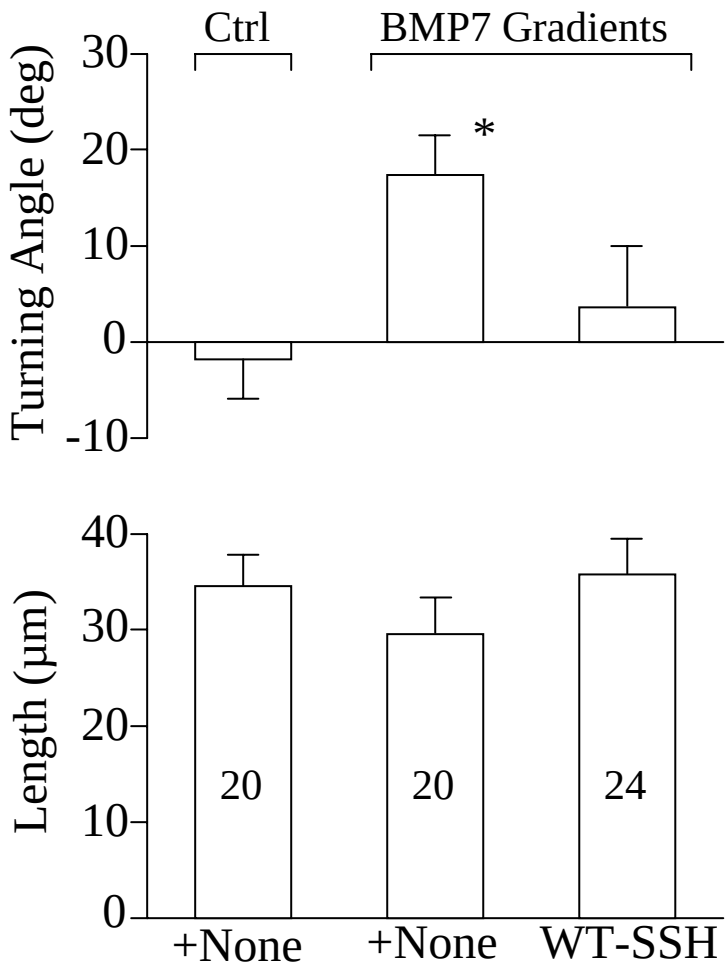

Supplemental figure 5. Attenuation of BMP7-induced attraction by over-expression of WT-XSSH in 4-8 hr cultures. The bar graphs summarize the average turning angles (top panel) and net extension (bottom panel) of different groups of growth cones with and without over-expression of WT-SSH. The BMP7 gradient was created by pressure ejection of 5 µM BMP7 from the micropipette. Numbers of growth cones examined for each condition are on bar graph. The over-expression of WT-SSH was achieved through blastomere mRNA injection (see Materials and Methods). The asterisk indicates a significant difference from the corresponding control ($p<0.05$, Mann-Whitney test). Numbers indicate the total number of growth cones examined for each condition.

Supplemental materials

Wen et al., http://www.jcb.org/cgi/content/full/jcb.200703055/DC1

Methods used for data presented in supplemental figures

RT-PCR analysis of BMPRII in *Xenopus* neural tube tissues. *Xenopus* embryos at 20–22 stages were dissected, the dorsal parts were subjected to 1 mg/ml collagenase for 30 min, and the neural tubes were separated from the myotome and notochord tissues. The first strand cDNA for PCR was synthesized from three neural tubes by the SuperScript III CellsDirect cDNA Synthesis kit (Invitrogen), and one tenth of the product was used in a 20-μl PCR system. Negative control for amplification was performed using the product without reverse transcriptase. We designed two sets of *Xenopus* BMPRII-specific primers as follows: primer set 1 (forward, 5′-AAGATGCAGAAGCCAGACT-3′; reverse, 5′-AGTTTTGGAGGCTTTCAAGC-3′), primer set 2 (forward, 5′-AGACGATTGATGATTGCTG-3′; reverse, 5′-CAGCGATTCCAGAACCACAA-3′; forward primers are located in the mRNA sequence of the kinase domain, and the reverse primers are located in the 3′ untranslated region). Conditions for the PCR reaction were 94°C for 30 s, 53°C for primer set 1 and 49°C for primer set 2 for 30 s, 72°C for 1 min 45 s for 40 cycles, and a 10-min 72°C final extension. PCR results were resolved on ethidium bromide–stained agarose gels, and the expected 1.7- and 1.8-kb bands showed the expression of *Xenopus* BMPRII mRNA. Our assays using both sets of primers did not detect the short form of BMPRII mRNA in *Xenopus* neural tubes.

Western blotting of ADF/cofilin. 20–22 stages of *Xenopus* embryos were homogenized in lysis buffer (50 mM Tris-HCl, pH 7.4, 150 mM NaCl, 1 mM EDTA, 1% Triton X-100, 1 mM PMSF, 1 mg/ml aprotinin, 1 mg/ml leupeptin, and 1 mg/ml pepstatin). The cell lysates were subjected to 15% SDS-PAGE and probed with XAC1 (electrophoresis 25:2,611; Shaw et al., 2004) or phosphocofilin 1 (Santa Cruz Biotechnology, Inc.) antibodies.

Live fluorescent imaging of cytoskeletal dynamics in growth cones. GFP–γ-actin and mRFP-EB3 were expressed in *Xenopus* neurons through the blastomere injection of mRNA molecules encoding these two constructs at the one- or two-cell stage. Neurons cultured from these embryos were examined by an imaging system consisting of an inverted microscope (TE2000; Nikon) equipped with a 60× NA 1.4 plan Apo oil immersion objective (Nikon), a CCD camera (SensiCam QE; Cooke Corp.), and a multispectral imager system (Dual-View; Optical Insights). To focally apply BMP7, a micropipette (1-μm opening) containing 5 μM of BMP7 solution was placed at 50 μm, 45° away from the growth cone. IPLab software (BD Biosciences) was used for imaging and recording.

Recorded time-lapse sequences were further processed by ImageJ software (NIH), including contrast enhancement, cropping, and resizing. We also used the Z-project function of ImageJ to collapse the time-lapse sequence to generate a single image that illustrates the distribution of GFP–γ-actin and mRFP-EB3. Because mRFP-EB3 appeared as discrete comets, Z project of the maximal intensity was able to capture all mRFP-EB3 comets over the entire time-lapse sequence. Therefore, the resultant image depicts the tracking map of mRFP-EB3 (+)*TIP*s over the time period. For GFP-actin, we used Z project of the intensity sum to create the image that contains the spatial distribution and intensity of GFP–γ-actin over the time period. As a result, increased actin-based protrusion on one side of the growth cone would generate more fluorescence intensity and/or a large area of GFP–γ-actin. Thus, overlaying the mRFP-EB3 map and the GFP-actin image can reveal any difference in the spatial distribution of these two cytoskeletal components.

Real-time PCR analysis of *Xenopus* TRPC1 and *Xenopus* BMPRII. *Xenopus* neural tubes were dissected from embryos at different stages. The first stand cDNA for real-time PCR (Fig. S1) was synthesized as described in the RT-PCR analysis section above. The following primers specific to *Xenopus* β-actin, *Xenopus* TRPC1, and *Xenopus* BMPRII were used: *Xenopus* β-actin (forward, 5′-AGCTGCCTGACGGACAAGT-3′; reverse, 5′-AATACCGCAGGATTCCATAC-3′), *Xenopus* TRPC1 (forward, 5′-AGCGAATCATGAGGACAAGGA-3′; reverse, 5′-GGCAGCGTGCATTTGTCA-3′), and *Xenopus* BMPRII (forward, 5′-GATCAAGATGCAGAAGCCAGACTA-3′; reverse, 5′-CCGTTCCCAAATCATCATGAG-3′).

Reference

Shaw, A.E., L.S. Minamide, C.L. Bill, J.D. Funk, S. Maiti, and J.R. Bamburg. 2004. Cross-reactivity of antibodies to actin-depolymerizing factor/cofilin family proteins and identification of the major epitope recognized by a mammalian actin-depolymerizing factor/cofilin antibody. *Electrophoresis.* 25:2611–2620.